

# Polyethylene Oxide and Silicon-Substituted Hydroxyapatite Composite: A Biomaterial for Hard Tissue Engineering in Orthopedic and Spine Surgery

## Abstract

**Background:** Tissue engineering and biomaterials have made it possible to innovate bone treatments for orthopedic and spine problems. The aim of this study is to develop a novel polyethylene oxide (PEO)/silicon-substituted hydroxyapatite (Si-HA) composite to be used as a scaffold for hard tissue engineering in orthopedic and spine procedures. **Materials and Methods:** The composite was fabricated through the electrospinning technique. The applied voltage (5 kV) and PEO concentration (5%) were fixed. Processing parameters such as the flow rates (20  $\mu$ l/min and 50  $\mu$ l/min), distances from capillary tube to the collector (130 mm and 180 mm), spinning time (10 min and 20 min), and concentration of Si-HA (0.2% and 0.6%) were explored to find the optimum conditions to produce fine composite fibers. **Results:** Scanning electron microscope images showed that 5% PEO, 5% PEO/0.2% Si-HA, and 5% PEO/0.6% Si-HA fibers were successively produced. Flow rates and working distances showed significant influence on the morphology of the polymeric and composite fibers. A high flow rate (50  $\mu$ l/min) and a larger working distance (180 mm) resulted in larger fibers. The comparison between the mean fiber diameter of 5% PEO/0.2% Si-HA and 5% PEO/0.6% Si-HA showed to be significantly different. As the Si-HA concentration increased, certain fibers were having particles of Si-HA that were not properly integrated into the polymer matrix. **Conclusions:** Synthesis of a novel biomaterial for hard tissue scaffold through electrospinning was successful. In general, PEO/Si-HA fibers produced have the desired characteristics to mimic the extracellular matrix of bone.

**Keywords:** Biomaterial, hard tissue engineering, orthopedics, polyethylene oxide, silicon-substituted hydroxyapatite, spine surgery, neurosurgery

## Introduction

The number of people suffering from bone defects is increasing considerably every year.<sup>[1]</sup> Not only are these conditions affecting the aging population, which is in constant growth, but they also represent a major health problem for the youth. Due to their high prevalence, bone diseases are associated with high morbidity, mortality, and a social and economic cost. The number of bone fractures is expected to reach 6.3 million worldwide by 2050.<sup>[2]</sup>

The most common treatments for bone fracture are surgical intervention and/or grafting. These treatment regimens are limited by the availability of the bone graft and the long healing process afterward. The need of orthopedic and spine surgeons for bone substitutes has led to a

high amount of research in the biomaterials and tissue engineering field.

The idea is to use a material which is biocompatible and bioactive to encourage natural tissue regeneration. In addition, the mechanical properties of the material should match the mechanical properties of the bone/joint/hard tissue being replaced to avoid stress shielding, which is a major cause of bone resorption.<sup>[3]</sup> However, the ideal biomaterial for the implant is still being investigated and orthopedic and spine surgeons insist on the need for new solutions.

The first generation of designed implants was composed of bioinert materials such as metals (stainless steel 316 L, cobalt–chromium alloy, titanium alloy: Ti-6%Al-4%V). This generation of bone implants was intended to match the physical

Nael Berri<sup>1,2</sup>,  
Jawad Fares<sup>2,3,4</sup>,  
Youssef Fares<sup>2,3</sup>

From the <sup>1</sup>Department of Mechanical Engineering, University College London, London, UK, <sup>2</sup>Neuroscience Research Center, <sup>3</sup>Department of Neurosurgery, Faculty of Medicine, Lebanese University, Beirut, Lebanon, <sup>4</sup>Department of Neurological Surgery, Feinberg School of Medicine, Northwestern University, Chicago, IL, USA

*Address for correspondence:*  
Dr. Nael Berri,  
Neuroscience Research Center,  
Faculty of Medicine, Lebanese  
University, Beirut, Lebanon.  
E-mail: [nael.berri@gmail.com](mailto:nael.berri@gmail.com)

### Access this article online

Website: [www.advbiores.net](http://www.advbiores.net)

DOI: 10.4103/abr.abr\_206\_17

### Quick Response Code:



**How to cite this article:** Berri N, Fares J, Fares Y. Polyethylene Oxide and Silicon-Substituted Hydroxyapatite Composite: A Biomaterial for Hard Tissue Engineering in Orthopedic and Spine Surgery. *Adv Biomed Res* 2018;7:117.

**Received:** December, 2017. **Accepted:** June, 2018.

This is an open access journal, and articles are distributed under the terms of the Creative Commons Attribution-NonCommercial-ShareAlike 4.0 License, which allows others to remix, tweak, and build upon the work non-commercially, as long as appropriate credit is given and the new creations are licensed under the identical terms.

For reprints contact: [reprints@medknow.com](mailto:reprints@medknow.com)

property of the replaced tissue,<sup>[4]</sup> as metal implants with highest volume porosity permit greater bone ingrowth.<sup>[5]</sup> The second generation of implants involved bioceramics, which are both biocompatible and bioactive and thus can promote a direct bond between the implant and the hard tissue. This “bioactive” characteristic has been made possible by the modification of bone implant surface with coating of bioactive materials such as bioceramics and/or surface topography modification. Although the first- and second-generation materials may be clinically effective, availability is a limitation. Therefore, further exploration in tissue engineering can present a new solution.

Bone tissue engineering strategies must be developed based on a good understanding of bone structure and bone dynamic (remodeling and repair). The development of fibrous matrices of a bioceramic-polymer composite offers a great potential in bone tissue engineering, as it allows us to mimic the mechanical properties and the biological composite of bone.

Synthetic polymer, polyethylene oxide (PEO), is a Food-and-Drug-Administration-approved polyether compound with many applications in medicine and/or industrial manufacturing.<sup>[6-9]</sup> Chemical properties of PEO are appropriate for scaffold fabrication. It is a nontoxic synthetic polymer and its by-products are easily excreted by the renal and hepatic pathways.<sup>[10]</sup> PEO is resistant to protein adhesion, and therefore, it does not interfere with cellular functions or target cells from the immune system.<sup>[10]</sup> PEO's nonimmunologic properties lower the risks of cytotoxic effects and material rejection, and have been found to suppress platelet adhesion and thrombus formation.<sup>[10]</sup> PEO is also hydrophilic, and therefore, it is easily dissolved in organic solvents and aqueous solutions and/or ethanol.<sup>[11]</sup> In addition, its excellent biocompatibility makes it an attractive candidate for scaffold materials of bone regeneration, and – when electrospun – it has been found to improve fiber properties and functionalities.<sup>[12]</sup>

In silicon-substituted hydroxyapatite (Si-HA), silicon is incorporated into the apatite crystal lattice by replacing the phosphate groups ( $\text{PO}_4^{3-}$ ) with silicate ions ( $\text{SiO}_4^{4-}$ ). The enhanced bioactivity and biocompatibility of this bioceramic attracted interest in the field of tissue engineering. The bioactivity response takes several days to occur with hydroxyapatite (HA), whereas those with silica-based glasses occur in lesser times.<sup>[13]</sup> The silicate ions incorporated into the HA lattice play an active role in bone formation and calcification.<sup>[14-17]</sup>

When comparing Si-HA granules to pure HA granules, bone growth was more remarkable in the presence of the incorporated silicate ions than with phase pure HA.<sup>[14]</sup> Reffitt *et al.*<sup>[18]</sup> reported that silicate ions in a biological environment appear to stimulate the differentiation of human osteoblast cells for the synthesis of Type I collagen

and other biochemical markers of bone cell maturation and bone formation.

The aim of this study is to develop a novel PEO/Si-HA composite to be used as a scaffold for hard tissue engineering in orthopedic and spine surgery. In the process, we will investigate the effects of processing parameters, such as using different distances between the needle tip and the grounded target, applied voltage, and concentration of Si-HA, on the morphology of the fibers. Typically, the composite fiber produced will mimic the topography and size of the extracellular matrix (ECM) of bone.

## Materials and Methods

### Preparing the setup

Electrospinning is a simple and inexpensive technique; its components (syringe pump, high voltage source, and collector) are cheap and easily available in the market. Its results have proved to be very competent in mimicking the nanoscale properties of the native ECM. This technique allows the production of polymer fibers with diameters in the range of micrometers down to a few nanometers.<sup>[19]</sup> This experiment has fixed parameters, which are applied voltage and polymer concentration, including the ratio of solvent. This experiment has also variable parameters: working distances, coating time, and flow rate.

### Preparing the polyethylene oxide polymer solution

PEO solutions of 5% w/v were electrospun. Polyethylene of 600,000 molecular weight was used in making the solution. The PEO polymer used was obtained from Sigma-Aldrich, a commercially available powder. PEO solutions were prepared by adding the PEO to deionized water and ethanol with a volume ratio water/ethanol = 1/3; which is the standardized method for the preparation of PEO fiber. Solutions were mixed by stirring for at least a day, at room temperature.

### Preparation of silicon-substituted hydroxyapatite

Si-HA was prepared using a precipitation method between a suspension of calcium hydroxide ( $\text{Ca}(\text{OH})_2$ ) and a solution of phosphoric acid ( $\text{H}_3\text{PO}_4$ ). Finally, tetraethyl orthosilicate,  $\text{C}_8\text{H}_{20}\text{O}_4\text{Si}$ , was added to  $\text{H}_3\text{PO}_4$  and mixed until the final suspension became homogenous.

### Sample preparation

Two different concentrations of PEO/Si-HA have been prepared by mixing PEO polymer and Si-HA with a solvent ratio of V (ethanol)/V (water) = 1/3:

- 5 (wt%) PEO/0.2 (wt%) Si-HA
- 5% PEO/0.6% Si-HA.

The pieces of glass that were fixed on the rotating collector were placed on a stub. The top of the stub was covered with a 12 mm Carbon Tab and the stubs were coated by gold using a sputter coating machine before studying them using the scanning electron microscope (SEM).

### Scanning electron microscope

Field emission SEM (SEM, JEOL JSM/6301F) was used for the imaging of the PEO fibers and composite, operating at an acceleration voltage of 5 kV.

### Fourier-transform infra-red spectroscopy

The structure of 5% PEO, 5% PEO/0.2% Si-HA, and 5% PEO/0.6% Si-HA was characterized by performing infrared (IR) spectral analysis. The analysis was performed using a Spectrum Two Fourier-transform IR (FTIR) (Perkin Elmer, UK). IR spectra were registered from 4500 to 450  $\text{cm}^{-1}$ .

### Statistical analysis

Two-tailed Student's *t*-test was used to discern the statistical difference between samples.  $P < 0.05$  was considered statistically significant.

### Fiber dimension characterization

Fiber diameter was assessed in PEO and PEO/Si-HA samples with a total of 50 measurements per sample.

For each sample, five measurements were taken along the length of one fiber to determine the average size of this fiber and take in account all the variations in size of the fiber. A total of 10 fibers per sample were measured. Quantitative image analysis of fiber diameters was performed using AutoCAD.

To be able to investigate variable parameters such as the effect of flow rates and working distances on the electrospun fiber, it was also necessary to have fixed parameters. Therefore, polymer composition and the solvent ratio were based on a previous experiment.<sup>[20]</sup> Fiber formability, effect of flow rate and working distance, morphology of the polymer fiber and composite fiber, and physical characterization were explored.

Initial investigation was needed to set up the applied voltage at a fixed parameter. To electrospun 5% PEO fibers, it was found that the most stable electrospinning jet was produced at 5 kV.

### Results

The relationship between flow rate and mean fiber diameter is direct at 10 min and at 20 min [Figure 1]. The mean fiber diameters of 5% PEO electrospun at 50  $\mu\text{l}/\text{min}$  were significantly larger than that electrospun at 20  $\mu\text{l}/\text{min}$ .

The effect of the working distance on the mean fiber diameter at 10 min and 20 min [Figure 1] was studied. At 50  $\mu\text{l}/\text{min}$ , the decrease in mean fiber diameter was significant as the working distance decreased from 180 mm to 130 mm. Comparison shows that there is no significant difference in mean fiber diameter at both 10 min and 20 min. However,  $P$  values indicate significant difference for the PEO fiber electrospun

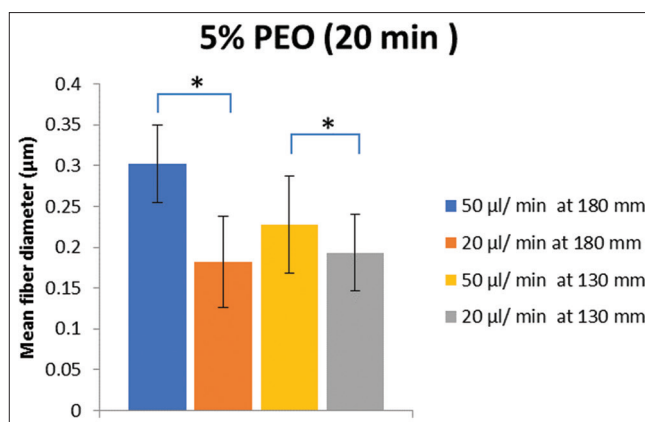


Figure 1: Mean fiber diameter of 5% polyethylene oxide fibers versus processing parameters (flow rate and working distance) at a spinning time of 20 min. \* $P < 0.05$

at the same working distance but different flow rates [Figure 2].

Polymeric fibers and composite fibers that were electrospun at 50  $\mu\text{l}/\text{min}$  and a working distance of 130 mm or 20  $\mu\text{l}/\text{min}$  and a working distance of 130 or 180 mm have mean fiber diameters of similar ranges [Figure 3]. However, a higher variation between the mean fiber diameter of 5% PEO and 5% PEO/0.2% Si-HA is observed at 50  $\mu\text{l}/\text{min}$  and a working distance of 180 mm.  $P$  values indicate significant difference between 5% PEO and 5% PEO/0.2% Si-HA in the 20  $\mu\text{l}/\text{min}$  at 180 mm, and in the 50  $\mu\text{l}/\text{min}$  at 130 mm and 180 mm, respectively. In addition, significant difference was observed between 5% PEO and 5% PEO/0.6% Si-HA [Figure 3]. The 5% PEO/0.6% Si-HA fibers electrospun at 20  $\mu\text{l}/\text{min}$  and at 180 mm were invalid and thus were not included.

High distribution of 5% PEO fibers in the form of a nonwoven mat resulted from electrospinning fibers of PEO for 20 min [Figure 4]. Whether the 5% PEO fiber were electrospun at 50  $\mu\text{l}/\text{min}$  or 20  $\mu\text{l}/\text{min}$  or at different working distances, they have shown to be uniform and to have a smooth surface [Figure 5]. Moreover, no beads on string were observed on the PEO fiber diameter.

In general, 5% PEO/0.2% Si-HA and 5% PEO/0.6% Si-HA show a uniform dispersion of Si-HA particles within the polyethylene polymer matrix. Overall, the Si-HA of different concentrations (0.2, 0.6 wt%) has been successfully incorporated into the PEO matrix. However, small bead-like structures are seen in some regions of the sample [Figure 6].

The “root-like” structure that was observed with 5% PEO Fiber was also present in 5%PEO/0.6% Si-HA [Figure 5]. Figure 7 shows ramifications along the length of the composite fiber.

In the functional group region (4000–1500  $\text{cm}^{-1}$ ), the absorption band between 2950 and 2800  $\text{cm}^{-1}$  indicates

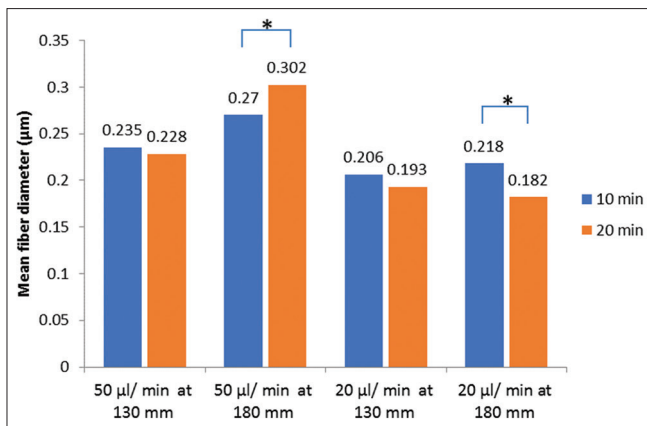


Figure 2: Mean fiber diameter of 5% polyethylene oxide at 10 min and 20 min, as per the different flow rates and working distances. \* $P < 0.05$

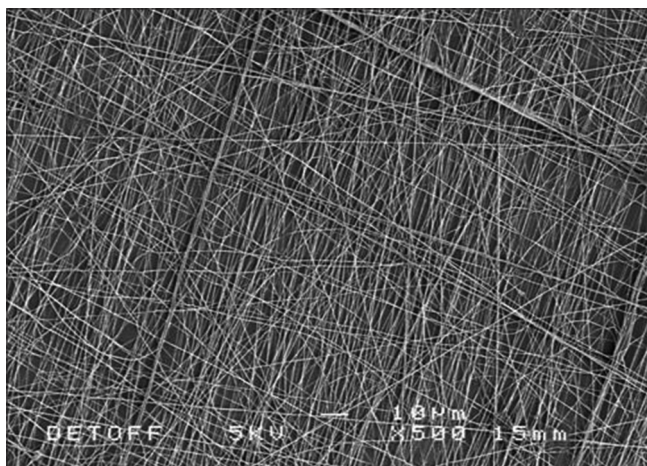


Figure 4: Scanning electron microscopy images of lower magnification of 5% polyethylene oxide electrospun at 130 mm and a flow rate of 50 µl/min

C-H stretching mode. The absorption band between 1050 and 1150  $\text{cm}^{-1}$  corresponds to C-O-C stretching. The absorption band present between 1260 and 1000  $\text{cm}^{-1}$  corresponds to C-O stretching. Absorption bands between 1300 and 1450  $\text{cm}^{-1}$  with peak at 1465  $\text{cm}^{-1}$  indicate C-H scissoring and bending, whereas and absorption between 2850 and 2960  $\text{cm}^{-1}$  with a peak at 2890  $\text{cm}^{-1}$  indicate C-H stretching. This result is coherent with the molecular structure of PEO ( $\text{CH}_2\text{CH}_2\text{O}$ ), where the methylene units are clearly revealed by the different peaks on the infrared spectrum. Moreover, these results correlate with the results of a similar study, whereby the molecular structure of PEO was investigated by X-ray diffraction and infrared absorption spectroscopic methods.<sup>[21]</sup>

We explored the infrared spectrum of PEO, 5% PEO/0.2% Si-HA and 5% PEO/0.6% Si-HA [Figure 8]. As observed, all the characteristic bands of ether (C-O-C stretching), alcohols (C-O stretching), alkanes (C-H stretching, scissoring, and bending), and hydroxyl (O-H stretching) were present on the spectrums of both 5% PEO/0.2% Si-HA and 5% PEO/0.6% Si-HA. This confirms the presence of

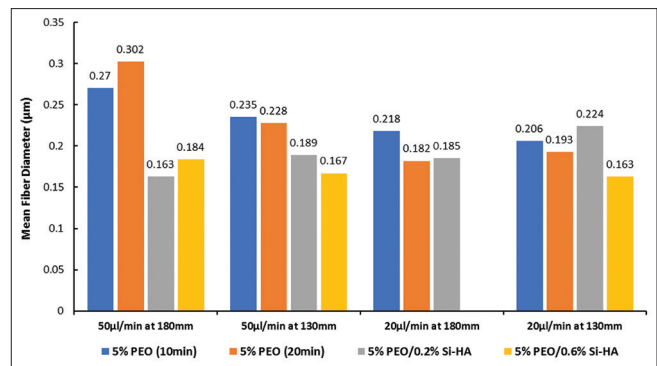


Figure 3: Comparison of the mean fiber diameters of 5% polyethylene oxide/0.2 silicon-substituted hydroxyapatite, 5% polyethylene oxide/0.6 silicon-substituted hydroxyapatite, and 5% polyethylene oxide (10 and 20 min).  $P$  values indicate significant difference between 5% polyethylene oxide and 5% polyethylene oxide/0.2% silicon-substituted hydroxyapatite in the 20 µl/min at 180 mm and in the 50 µl/min at 130 mm and 180 mm, respectively. Significant difference was also observed between 5% polyethylene oxide and 5% polyethylene oxide/0.6% silicon-substituted hydroxyapatite. Note: The 5% polyethylene oxide/0.6% silicon-substituted hydroxyapatite fibers electrospun at 20 µl/min and at 180 mm were invalid and thus were not included

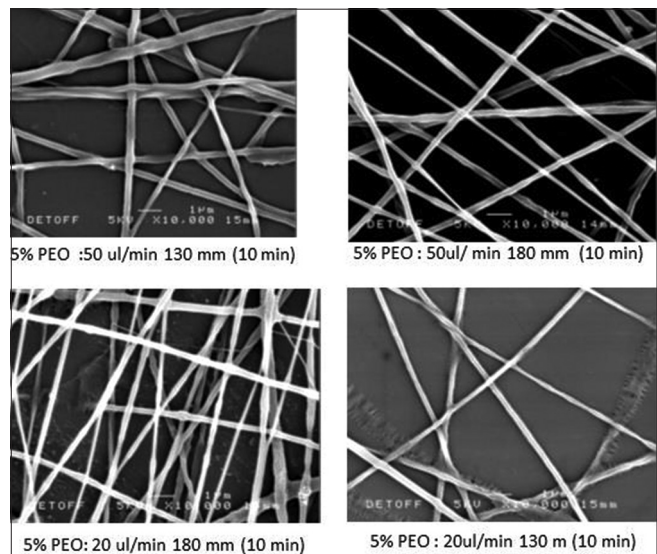
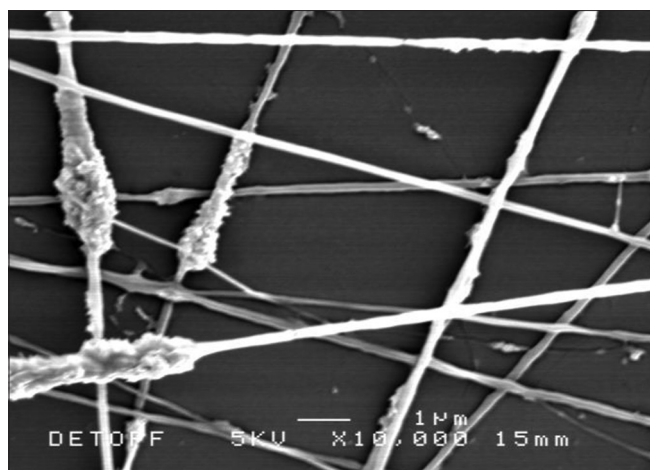


Figure 5: Scanning electron microscopy pictures of 5% polyethylene oxide at different processing parameters, while spinning for 10 min

PEO in the composite. However, PEO/Si-HA spectrums show additional absorption bands when compared to the PEO spectrum; characteristic peaks that appear at 1030, 633, 600, and 564  $\text{cm}^{-1}$  wavelengths are only present on PEO/Si-HA-composite spectra. The absorption band between 450 and 660  $\text{cm}^{-1}$  with peaks at 564, 600, and 633  $\text{cm}^{-1}$  wavelengths is characteristic of  $\text{PO}_4^{2-}$  bands. Indeed, peaks at 600 and 564  $\text{cm}^{-1}$  represent the triply degenerated bending mode of the O-P-O bonds of the phosphate group. The peak at 630  $\text{cm}^{-1}$  indicates hydroxyl stretch bands. Moreover, an additional proof of the presence of  $\text{PO}_4^{2-}$  is the peak at 1030  $\text{cm}^{-1}$  which is characteristic to triply degenerated asymmetric stretching mode of the P-O bond of the phosphate group. The presence of  $\text{SiO}_4^{4-}$  groups



**Figure 6:** Scanning electron microscopy image of 5% polyethylene oxide/0.6% silicon-substituted hydroxyapatite showing bioceramic particles not fully integrated in the polymer matrix

in the apatite structure is represented on the spectrum by the peak at  $490\text{ cm}^{-1}$ .<sup>[22]</sup>

A higher transmittance of the band between  $450$  and  $660\text{ cm}^{-1}$  with peaks at  $564$ ,  $600$ , and  $633\text{ cm}^{-1}$  wavelengths characteristic of  $\text{PO}_4^{2-}$  is observable on 5% PEO/0.2% Si-HA when compared to 5% PEO/0.6% Si-HA [Figure 8]. The O-P-O bond peak appears at  $62.4\text{T\%}$  on the 5% PEO/0.2% Si-HA spectrum and  $71.54\text{T\%}$  on 5% PEO/0.6% Si-HA spectrum. The fact that the characteristic band of  $\text{PO}_4^{2-}$  is in higher transmittance confirms the higher concentration of Si-HA in 5% PEO/0.6% Si-HA.

## Discussion

### Effect of the processing parameters on the 5% polyethylene oxide fibers

It is known that the flow rate influences the morphology of the electrospun fiber; it will determine the quantity of the polymeric solution available to be electrospun. Therefore, increasing the flow rates while maintaining the Taylor cone will provide a higher volume drawn from the needle tip, and lead to a lower amount of the solvent evaporating, eventually resulting in larger fibers.<sup>[23]</sup> In certain cases, a flow rate that is too high resulted in beading because fibers did not have enough time to dry before reaching the collector. However, in this experiment, no beads were formed which supports the use of this biomaterial for hard tissue engineering, as we want the fiber to be uniform.

### Significant difference observed at different spinning times

An unexpected significant difference was found for PEO fibers electrospun at 10 min and 20 min. One possible explanation is that, in the 10-min difference, the density of fiber produced changes. Therefore, a substrate that has been coated in 20 min has a higher density of fiber overlapped and compressed than at 10 min, and thus it is open to more variation of size.

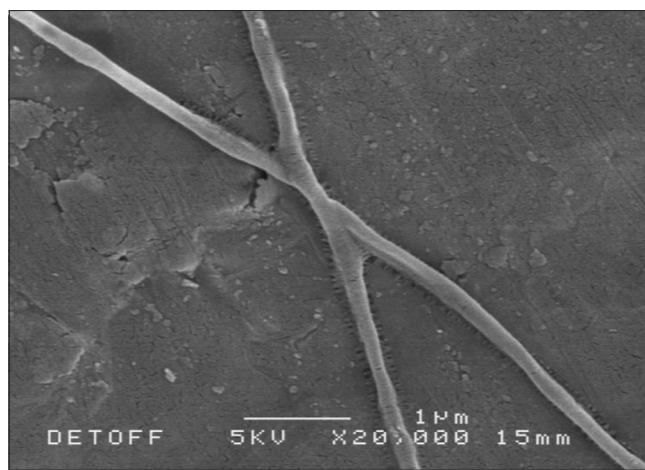


**Figure 7:** The “root-like” shape of 5% polyethylene oxide/0.6% silicon-substituted hydroxyapatite at a flow rate of  $20\text{ }\mu\text{l/min}$  and a working distance of  $130\text{ mm}$

### Significant difference of the mean fiber diameter of 5% polyethylene oxide/0.2% silicon-substituted hydroxyapatite and 5% polyethylene oxide/0.6% silicon-substituted hydroxyapatite

The comparison between the mean fiber diameter of 5% PEO/0.2% Si-HA and 5% PEO/0.6% Si-HA showed to be significantly different, even when they were electrospun at the same processing parameters. The only different variable between the two samples was the concentration of Si-HA. In fact, it was observed that certain fibers had particles of Si-HA that were not properly integrated into the polymer matrix. As the concentration increased (from 0.2% to 0.6%), the incidence of this unincorporated material was higher.

### Ambient parameters

Ambient parameters such as room temperatures and humidity may have played a role in error. It has been suggested that high humidity could condense the water on the surface of the electrospun fiber.<sup>[24]</sup> Water condensation might interfere with the evaporation rate of the solvent. In addition, depending on the chemical nature of the polymer, high humidity would increase the evaporation rate, whereas low humidity would decrease the rate.<sup>[25]</sup> Therefore, humidity has the potential to make the diameter of the fiber thicker or thinner and that depends not only on the relative humidity but also on the chemical nature of the polymer.<sup>[25]</sup> Moreover, investigation has been made on the effect of humidity on PEO and the results showed that as the humidity increases, the mean fiber diameter of PEO decreases.<sup>[26,27]</sup> Therefore, even though the processing parameters remain the same, the fiber diameter could differ with changes in humidity.

Temperature also influences the electrospun fiber; however, it does not depend on the chemical properties of the solvent. In fact, as the temperature rises, the fiber diameter increases due to a higher rate of solvent evaporation.<sup>[25]</sup>

Therefore, factors such as lighting (that generates heat) could have affected the mean fiber diameter by increasing the evaporation rate and leading to thinner fibers than expected. However, ambient parameters must have had only a small effect on the experimental errors as the experiment was performed in a controlled environment.

### Measurement accuracy

AutoCAD software enables accurate measurement of the electrospun fiber at a scale of 0.1  $\mu\text{m}$ . However, as the magnification increases the delimitation of the fibers are more difficult to determine [Figure 9]. For accuracy purposes, observational error of one fiber has been determined by measuring the fiber diameter in different aspects at a precise point:

- One measurement was taken in the high concentration pixel zone. This zone is characterized by a white color on the picture, which gives the minimal value
- One measurement was taken in the low concentration pixel zone. This zone is characterized by a gray color on the picture, which gives the maximal value
- Three measurements in the intermediate zone (between high concentration pixel zone and low concentration pixel zone).

These five measurements gave a standard deviation of 0.015  $\mu\text{m}$ , which corresponds to an error in the range of 14%. This standard deviation, which may vary from one observation to another, remains low, and proves that whether the fiber diameter is delimited from one zone to

another, it will not have a remarkable change on the mean fiber diameter.

FTIR was used to study the physical characterization group of PEO and PEO/Si-HA solutions. The characteristic groups found on PEO spectrum were also found on the composite. Moreover, the characteristic groups of  $\text{PO}_4^{3-}$  and  $\text{SiO}_4^{4-}$  from mineral Si-HA were distinguished on the PEO/Si-HA spectra; this confirms the presence of Si-HA in the composites.

FTIR was able to determine a greater amount of Si-HA in one of the mixture composite confirming the quality and consistency of the samples before the experiment. However, the literature has mentioned three bands (490, 760 and 890  $\text{cm}^{-1}$ ) for the presence of Silo groups, whereas only one peak was found in our PEO/0.2% Si-HA and PEO/0.6% Si-HA composites. The presence of bands generated between 450 and 760  $\text{cm}^{-1}$  with characteristic peaks of  $\text{PO}_4^{3-}$  seems to be the cause of the disappearance of the two missing bands attributed to Si-O-Si vibration from the PEO/Si-HA composite.

### Optimal characteristic of the composite fibers

Electrospinning technique has successfully produced smooth and uniform biopolymer/bioceramic fibers. No bead formation was observed, even for the thinner fibers. This is a positive result as beads have shown to cause limited cell adhesion. Moreover, the fiber randomly electrospun on the collector formed pores. The presence of pores is an important feature for scaffolds in bone tissue engineering as it stimulates cell proliferation once the cells are attached.

### Conclusions

Synthesis of a novel biomaterial for hard tissue scaffold through electrospinning was successful. PEO/Si-HA fibers produced have the desired characteristics to mimic ECM of bone. The mean fiber diameter of this novel composite

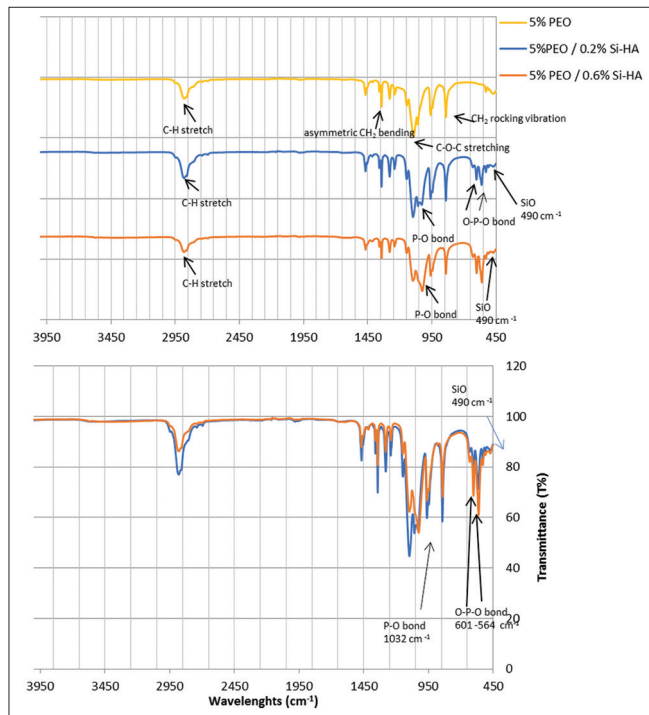


Figure 8: Comparison of the spectra of 5% polyethylene oxide, 5% polyethylene oxide/0.2% silicon-substituted hydroxyapatite, and 5% polyethylene oxide/0.6% silicon-substituted hydroxyapatite

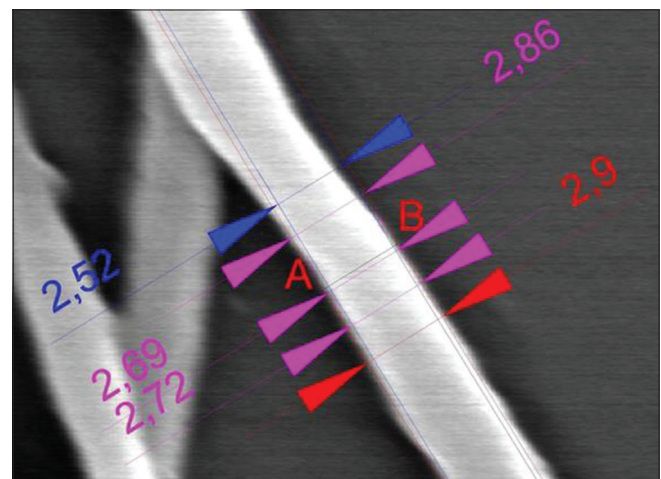


Figure 9: Method of measurement using auto computer-aided design software. Different zones are observed. One zone characterized by a white color and shows the high-density pixels, whereas the zone characterized by a gray color shows the low-density pixels

is in the desired range and the random distribution of the PEO/Si-HA fiber on the substrate permitted the formation of pores, which is an important property for bone tissue formation. Further trials and experimentation are needed before using this novel composite for biomedical applications in orthopedic and spine surgeries.

### Acknowledgments

We would like to thank Dr. Jie Huang for providing the setting to conduct the experiments, and for her supervision and assistance all throughout the work of this project.

### Financial support and sponsorship

Nil.

### Conflicts of interest

There are no conflicts of interest.

### References

1. National Osteoporosis Society. A Strategy to Reduce the Impact of Osteoporosis and Fragility Fractures in England; 2009. Available from: <http://www.nos.org.uk/document.doc?id=491>. [Last accessed on 2018 Jun 20].
2. Cooper C, Campion G, Melton LJ 3<sup>rd</sup>. Hip fractures in the elderly: A world-wide projection. *Osteoporos Int* 1992;2:285-9.
3. Huiskes R, Weinans H, van Rietbergen B. The relationship between stress shielding and bone resorption around total hip stems and the effects of flexible materials. *Clin Orthop Relat Res* 1992;274:124-34.
4. Hench LL, Polak JM. Third-generation biomedical materials. *Science* 2002;295:1014-7.
5. Archibeck MJ, Berger RA, Jacobs JJ, Quigley LR, Gitelis S, Rosenberg AG, *et al.* Second-generation cementless total hip arthroplasty. Eight to eleven-year results. *J Bone Joint Surg Am* 2001;83-A: 1666-73.
6. Griffith LG. Polymeric biomaterials. *Acta Mater* 2000;48:263-77.
7. Peppas NA, Hilt JZ, Khademhosseini A, Langer R. Hydrogels in biology and medicine: From molecular principles to bionanotechnology. *Adv Mater* 2006;18:1345-60.
8. Gutowska A, Jeong B, Jasionowski M. Injectable gels for tissue engineering. *Anat Rec* 2001;263:342-9.
9. Hoffman AS. Hydrogels for biomedical applications. *Adv Drug Deliv Rev* 2012;64:18-23.
10. Nagaoka S, Nakao A. Clinical application of antithrombogenic hydrogel with long poly (ethylene oxide) chains. *Biomaterials* 1990;11:119-21.
11. Liang D, Hsiao BS, Chu B. Functional electrospun nanofibrous scaffolds for biomedical applications. *Adv Drug Deliv Rev* 2007;59:1392-412.
12. Duan B, Dong C, Yuan X, Yao K. Electrospinning of chitosan solutions in acetic acid with poly(ethylene oxide). *J Biomater Sci Polym Ed* 2004;15:797-811.
13. Zhong J, Greenspan DC. Processing and properties of sol-gel bioactive glasses. *J Biomed Mater Res* 2000;53:694-701.
14. Patel N, Best SM, Bonfield W, Gibson IR, Hing KA, Damien E, *et al.* A comparative study on the *in vivo* behavior of hydroxyapatite and silicon substituted hydroxyapatite granules. *J Mater Sci Mater Med* 2002;13:1199-206.
15. Pietak AM, Reid JW, Stott MJ, Sayer M. Silicon substitution in the calcium phosphate bioceramics. *Biomaterials* 2007;28:4023-32.
16. Porter AE, Buckland T, Hing K, Best SM, Bonfield W. The structure of the bond between bone and porous silicon-substituted hydroxyapatite bioceramic implants. *J Biomed Mater Res A* 2006;78:25-33.
17. Thian ES, Huang J, Best S, Barber ZH, Bonfield W. Fast apatite-forming ability of magnetron co-sputtered silicon-containing hydroxyapatite (Si-HA) thin films. *Key Eng Mater* 2005;284:445-8.
18. Reffitt DM, Ogston N, Jugdaohsingh R, Cheung HF, Evans BA, Thompson RP, *et al.* Orthosilicic acid stimulates collagen type I synthesis and osteoblastic differentiation in human osteoblast-like cells *in vitro*. *Bone* 2003;32:127-35.
19. Subbiah T, Bhat GS, Tock RW, Parameswaran S, Ramkumar SS. Electrospinning of nanofibers. *J Appl Polym Sci* 2005;96:557-69.
20. Son WK, Youk JH, Park WH. Preparation of ultrafine oxidized cellulose mats via electrospinning. *Biomacromolecules* 2004;5:197-201.
21. Tadokoro H, Chatani Y, Yoshihara T, Tahara S, Murahashi S. Structural studies on polyethers, [-(CH<sub>2</sub>) m-O] n. II. Molecular structure of polyethylene oxide. *Macromol Chem Phys* 1964;73:109-27.
22. Aminian A, Solati-Hashjin M, Samadikuchaksaraei A, Bakhshi F, Gorjipour F, Farzadi A, *et al.* Synthesis of silicon-substituted hydroxyapatite by a hydrothermal method with two different phosphorous sources. *Ceram Int* 2011;37:1219-29.
23. Zong X, Kim K, Fang D, Ran S, Hsiao BS, Chu B. Structure and process relationship of electrospun bioabsorbable nanofiber membranes. *Polymer* 2002;43:4403-12.
24. Magalski A, Adamson P, Gadler F, Böehm M, Steinhaus D, Reynolds D, *et al.* Continuous ambulatory right heart pressure measurements with an implantable hemodynamic monitor: A multicenter, 12-month follow-up study of patients with chronic heart failure. *J Card Fail* 2002;8:63-70.
25. De Vrieze S, Van Camp T, Nelvig A, Hagström B, Westbroek P, De Clerck K. The effect of temperature and humidity on electrospinning. *J Mater Sci Mater Med* 2009;44:1357.
26. Yang Y, Jia Z, Li Q, Guan Z. Experimental investigation of the governing parameters in the electrospinning of polyethylene oxide solution. *IEEE Trans Dielectr Electr Insul* 2006;13:580-5.
27. Tripatanasuwana S, Zhong Z, Reneker DH. Effect of evaporation and solidification of the charged jet in electrospinning of poly (ethylene oxide) aqueous solution. *Polymer* 2007;48:5742-6.